

Supplementary Information

Charge Optimization Induces Reconstruction via Compounding Ni(OH)₂ and CoP: A Novel Route to Construct Electrocatalysts for Overall water splitting

Hao Yin,[‡] Bingxian Wu,[‡] Xueyang Leng, Hong Gao, and Jing Yao*

School of Physics and Electronic Engineering, Key Laboratory for Photonic and Electronic Bandgap Materials, Ministry of Education, Harbin Normal University, Harbin 150025, China

*Corresponding author E-mail: yaojing@hrbnu.edu.cn (J. Yao)

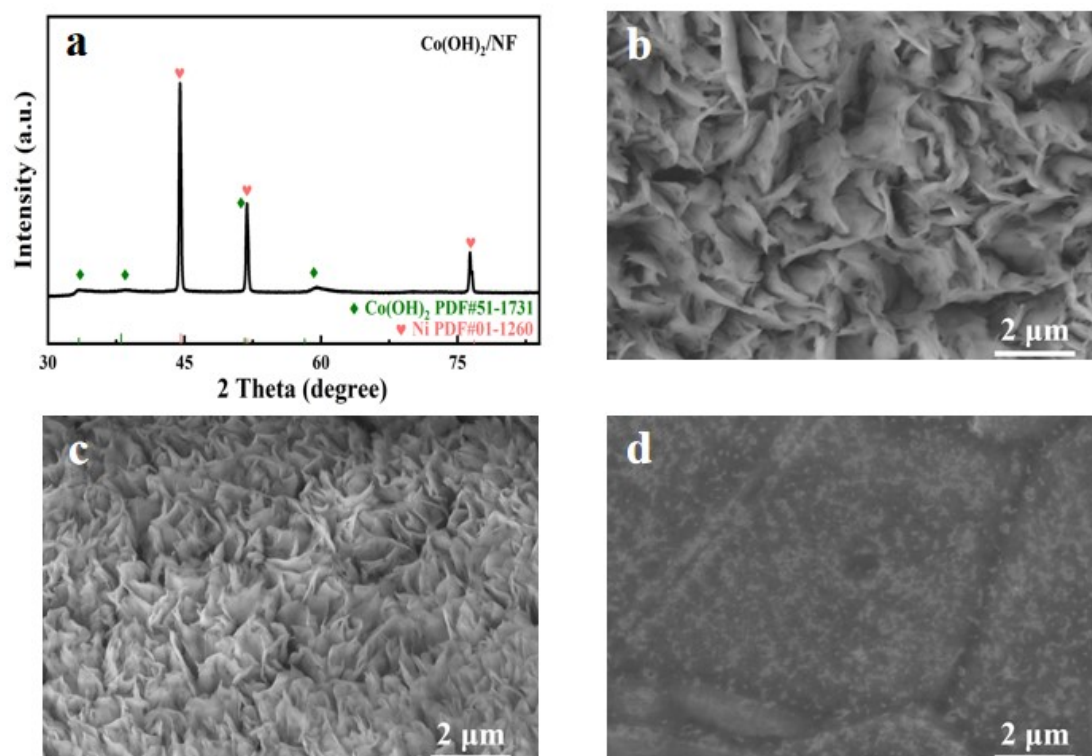


Figure S1. (a) XRD patterns of Co(OH)₂/NF, (b-d) SEM images of Co(OH)₂/NF with the deposition time of 5 minutes, 10 minutes and 20 minutes, respectively.

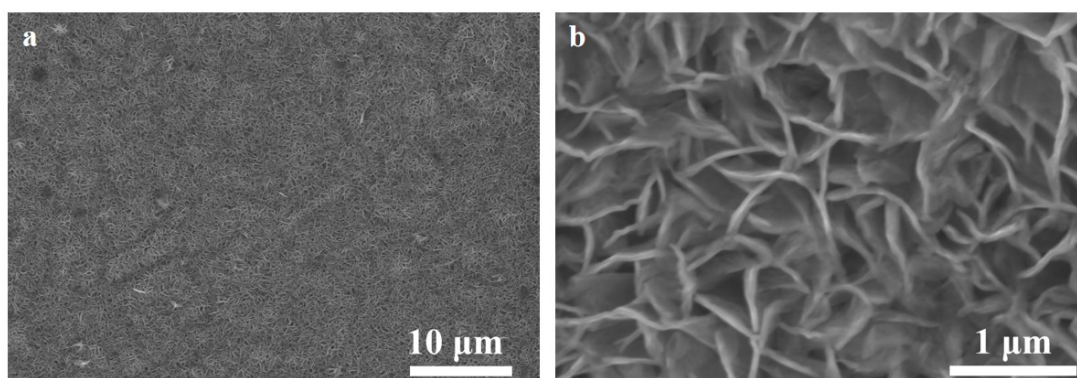


Figure S2. (a) Low and (b) high-resolution SEM images of CoP.

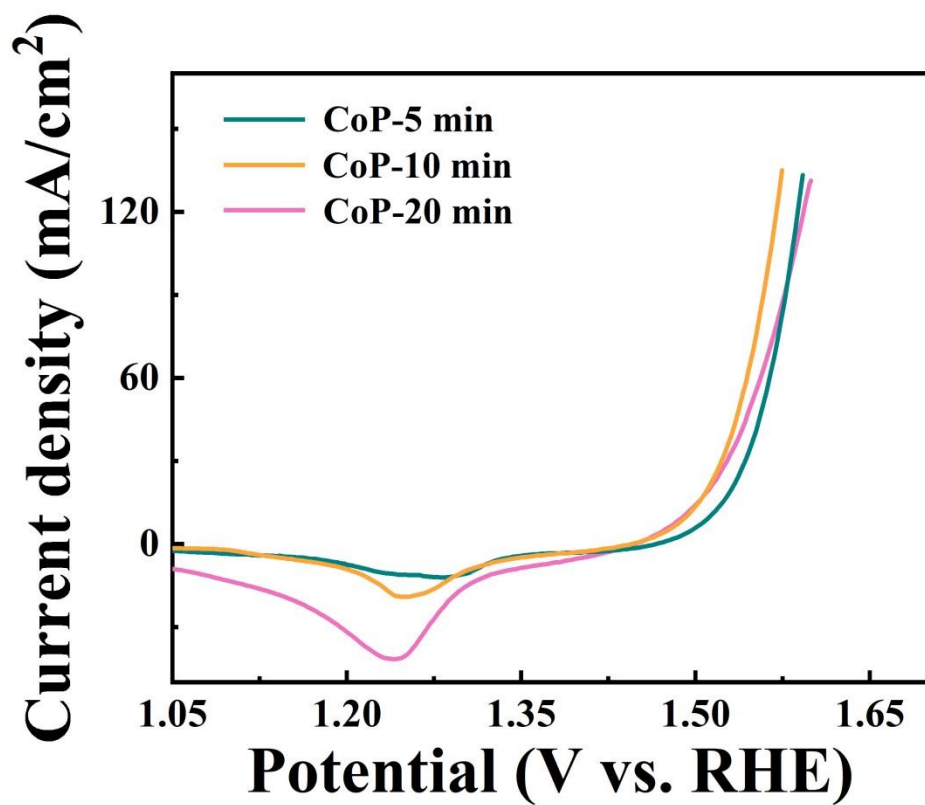


Figure S3. OER LSV curves of CoP with different description time.

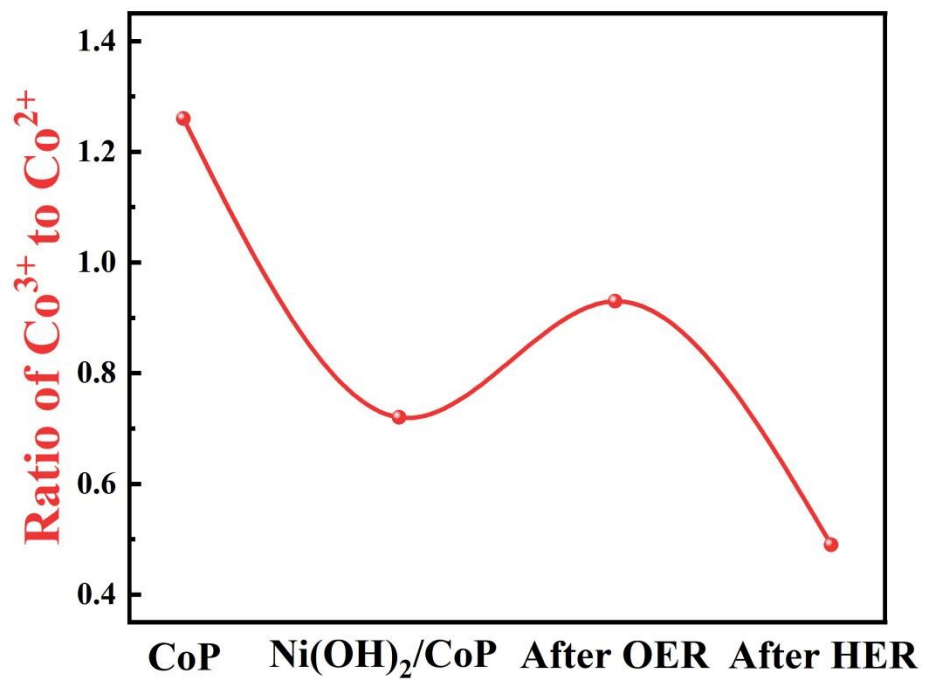


Figure S4. The ratio of Co³⁺ to Co²⁺ in CoP, Ni(OH)₂/CoP, Ni(OH)₂/CoP after OER and Ni(OH)₂/CoP after HER.

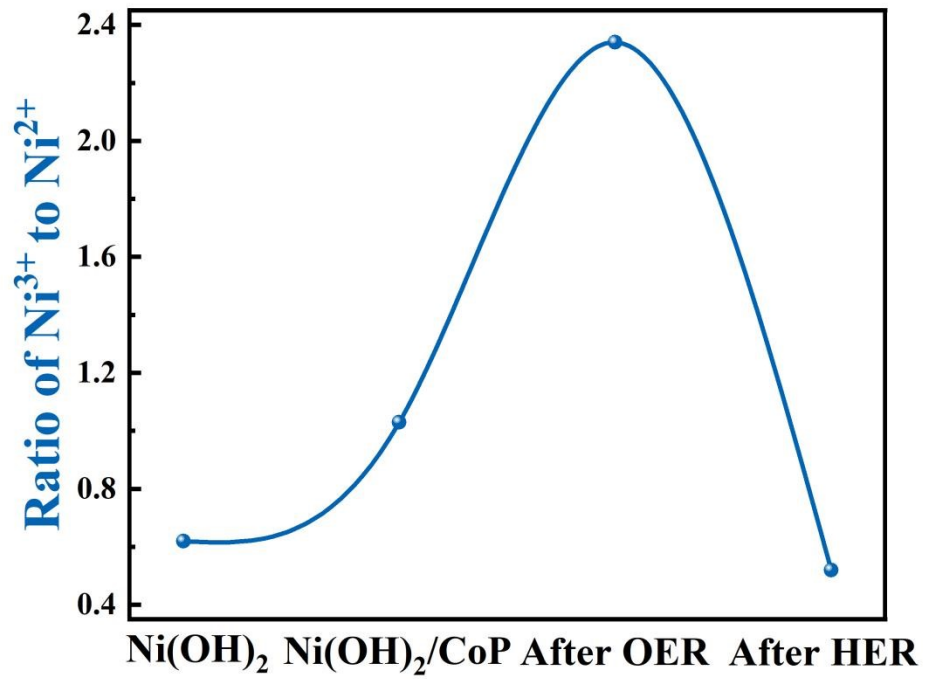


Figure S5. The ratio of Ni³⁺ to Ni²⁺ in Ni(OH)₂, Ni(OH)₂/CoP, Ni(OH)₂/CoP after OER and Ni(OH)₂/CoP after HER.

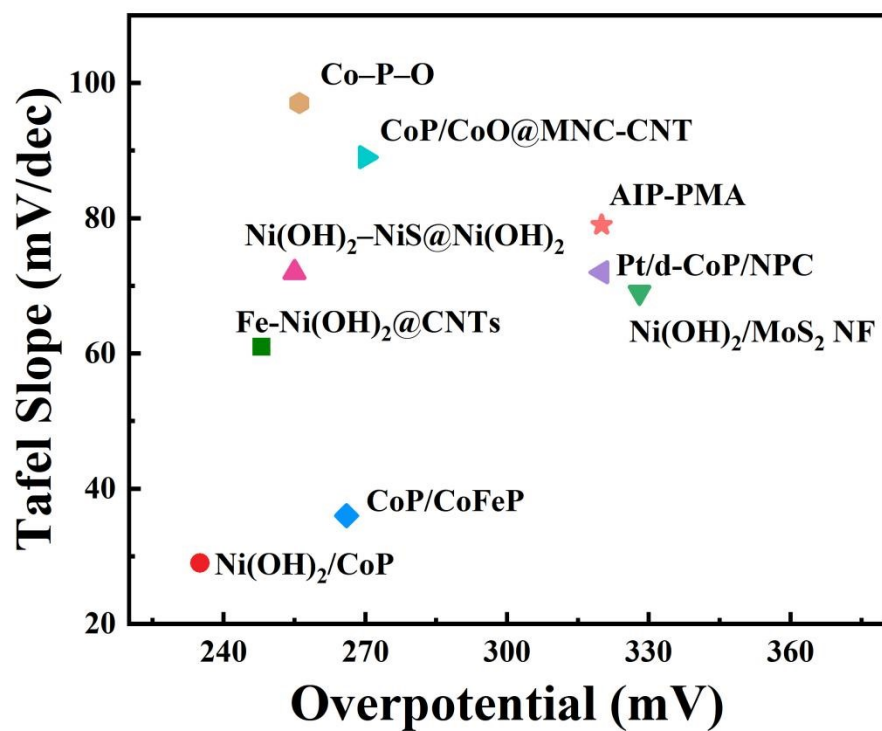


Figure S6. Overpotential and Tafel slope of Ni(OH)₂/CoP and the reported noble-free electrocatalysts for OER, respectively.

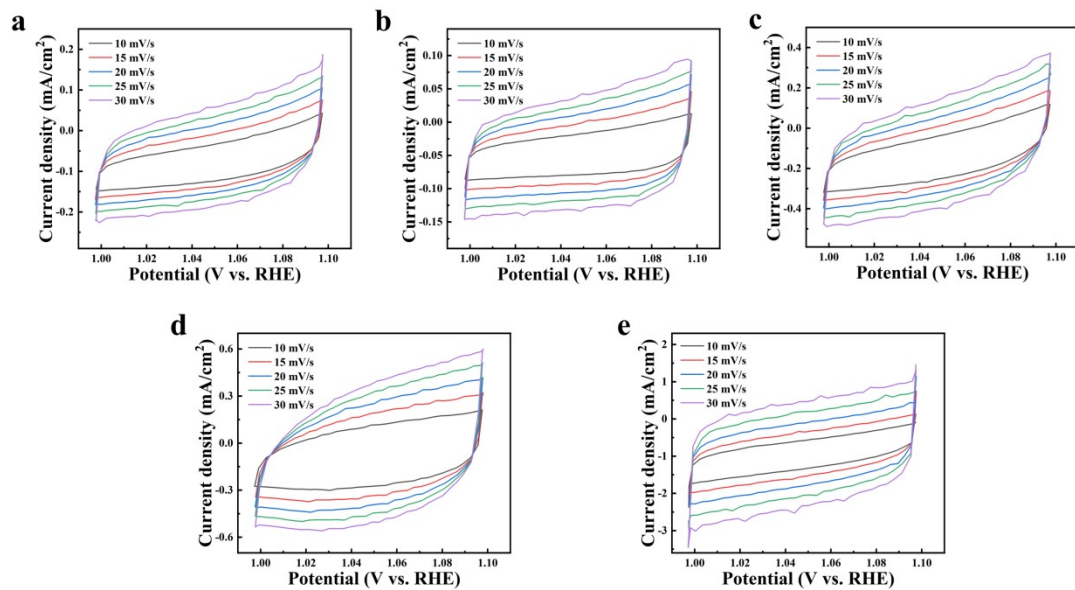


Figure S7. CV curves at different scan rates between 1.00 and 1.10 V vs. RHE for (a) CoP, (b) Ni(OH)₂, (c) Ni(OH)₂/CoP-5, (d) Ni(OH)₂/CoP-10 and (e) Ni(OH)₂/CoP-20, respectively.

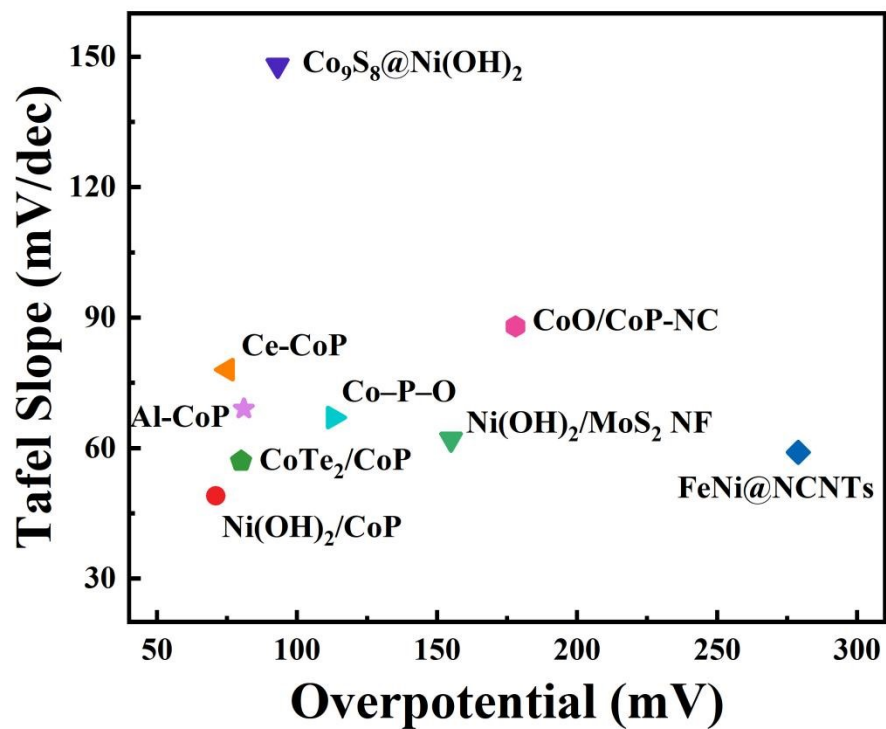


Figure S8. Overpotential and Tafel slope of $\text{Ni}(\text{OH})_2/\text{CoP}$ and the reported noble-free electrocatalysts for HER, respectively.

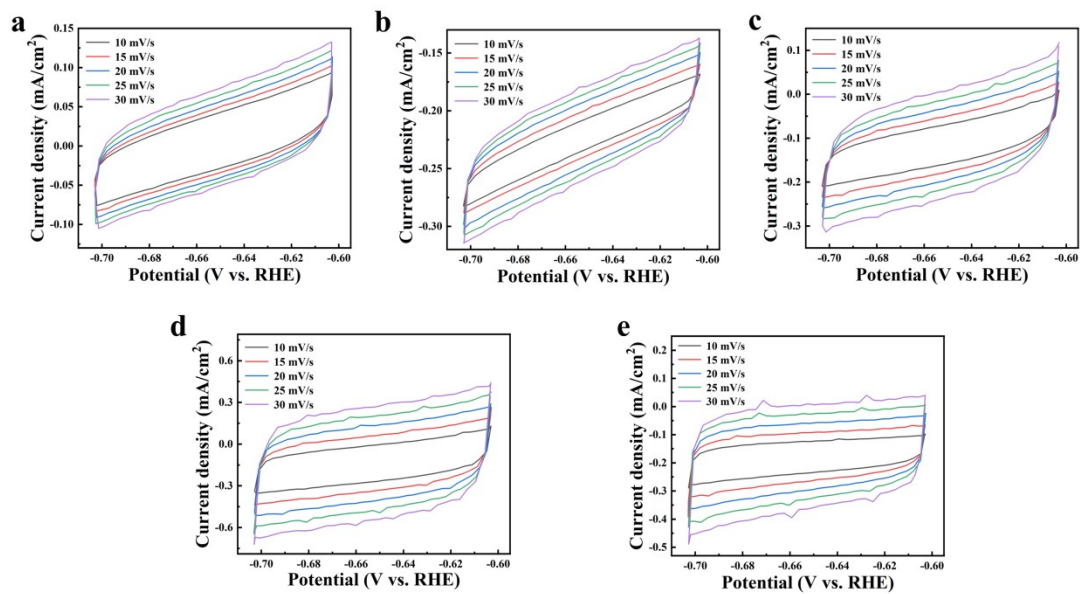


Figure S9. CV curves at different scan rates between -0.70 and -0.60 V vs. RHE for (a) CoP, (b) Ni(OH)₂, (c) Ni(OH)₂/CoP-5, (d) Ni(OH)₂/CoP-10 and (e) Ni(OH)₂/CoP-20, respectively.

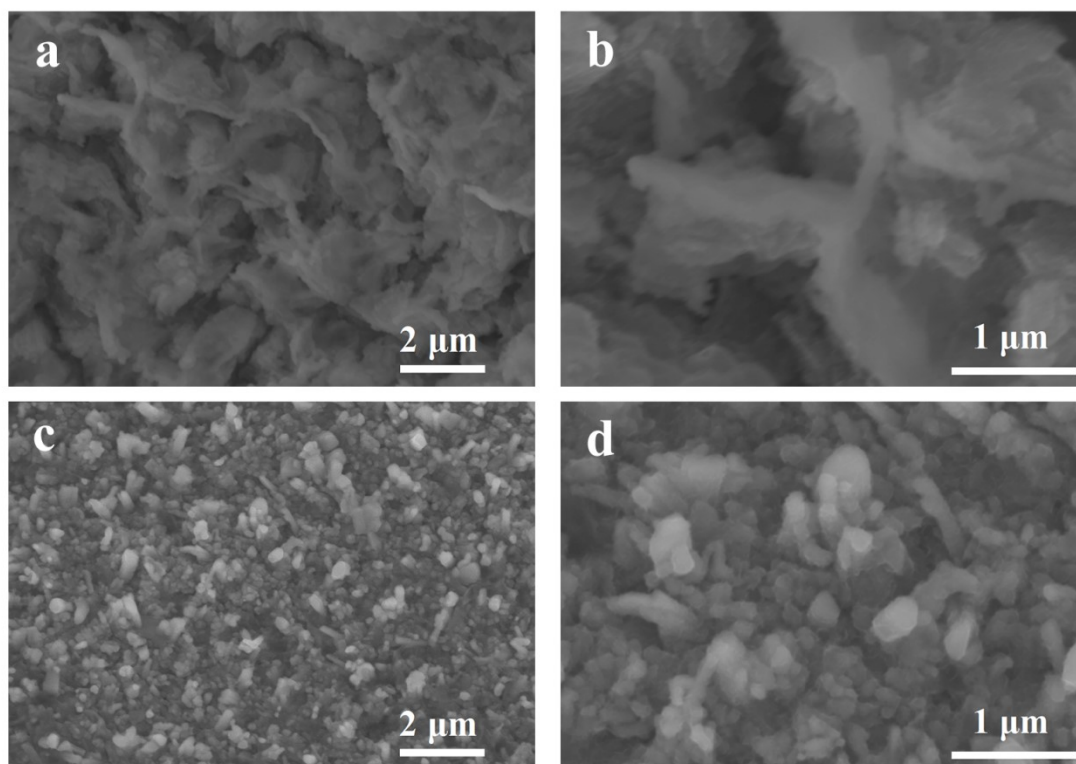


Figure S10. Low and high-resolution SEM images of (a,b) Ni(OH)₂/CoP-10 after OER and (c,d) Ni(OH)₂/CoP-10 after HER.

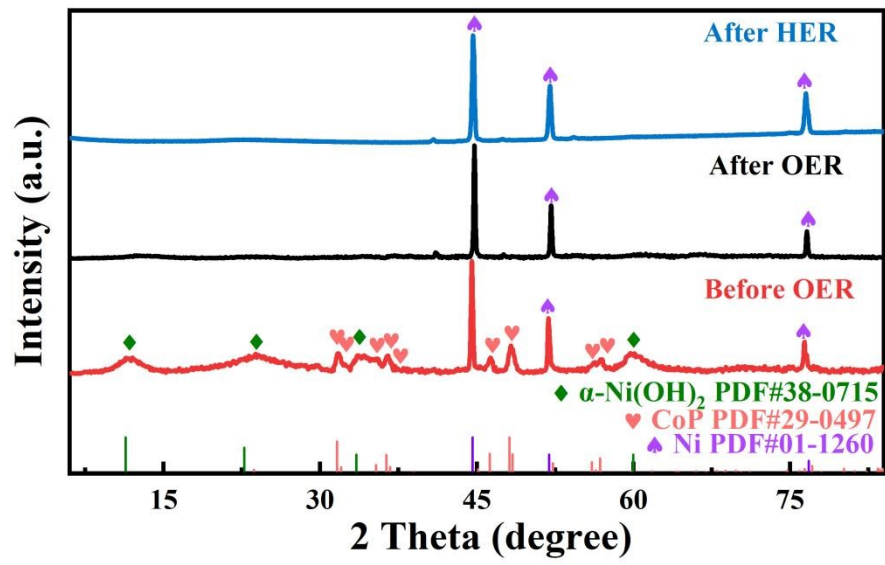


Figure S11. XRD patterns of Ni(OH)₂/CoP-10 before OER, after OER and after HER.

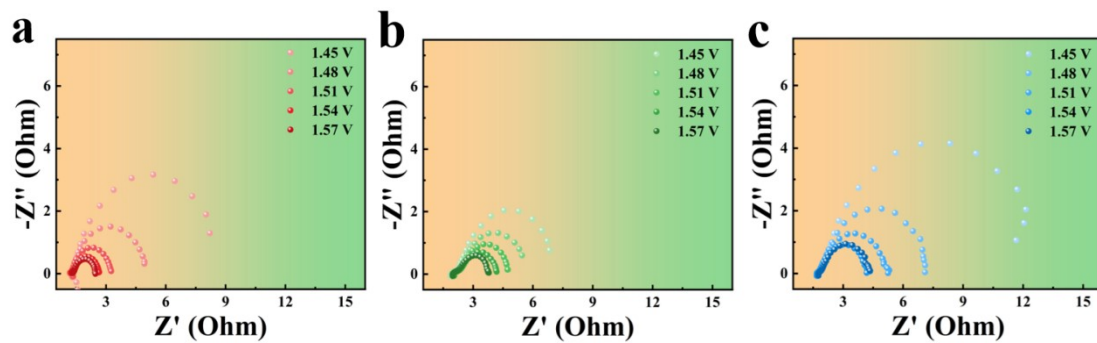


Figure S12. Situ EIS plots of (a) Ni(OH)₂/CoP, (b) CoP and (c) Ni(OH)₂.

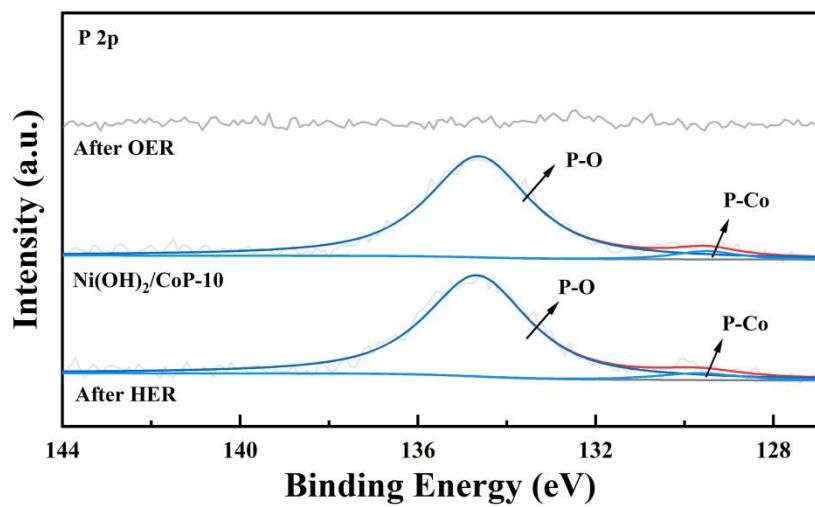


Figure S13. P 2p XPS spectra of Ni(OH)₂/CoP-10, Ni(OH)₂/CoP-10 after OER and Ni(OH)₂/CoP-10 after HER.

Table S1. Overpotential and Tafel slope of the reported noble-free electrocatalysts for OER (η_{10} , η_{50} and η_{100} : overpotential at 10, 50 and 100 mA/cm², respectively).

Catalysts	Electrolyte	η (mV)	Tafel Slope (mV/dec)	References
Ni(OH)₂/CoP	1M KOH	η_{10}=235 η_{50}=266 η_{100}=283	29	This work
Fe-Ni(OH) ₂ @CNTs	1M KOH	η_{10} =248	61	1
Ni(OH) ₂ -NiS@Ni(OH) ₂	1M KOH	η_{10} =255	72	2
Se-NiS ₂	1M KOH	η_{50} =343	140	3
Ni(OH) ₂ /MoS ₂ NF	1M KOH	η_{10} =328	69	4
Ni/Ni(OH) ₂ @NM	1M KOH	η_{100} =337	47	5
CoP/CoFeP	1M KOH	η_{10} =266	36	6
Pt/d-CoP/NPC	1M KOH	η_{10} =320	72	7
CoP/CoO@MNC-CNT	1M KOH	η_{10} =270	89	8
Co-P-O	1M KOH	η_{10} =256	97	9
AIP-PMA	1M KOH	η_{10} =320	79	10

Table S2. Overpotential and Tafel slope of the reported noble-free electrocatalysts for HER (η_{10} , η_{50} and η_{100} : overpotential at 10, 50 and 100 mA/cm², respectively).

Catalysts	Electrolyte	η (mV)	Tafel Slope (mV/dec)	References
Ni(OH)₂/CoP	1M KOH	$\eta_{10}=71$ $\eta_{50}=113$ $\eta_{100}=145$	49	This work
Ni(OH) ₂ /MoS ₂ NF	1M KOH	$\eta_{10}=155$	62	4
Ni/Ni(OH) ₂ @NM	1M KOH	$\eta_{100}=164$	90	5
Co-P-O	1M KOH	$\eta_{10}=113$	67	9
Co ₉ S ₈ @Ni(OH) ₂	1M KOH	$\eta_{10}=93$	148	11
FeNi@NCNTs	1M KOH	$\eta_{10}=279$	59	12
Al-CoP	1M KOH	$\eta_{10}=75$	78	13
CoTe ₂ /CoP	1M KOH	$\eta_{10}=80$	57	14
NiZn@C-CoP	1M KOH	$\eta_{10}=78$	57	15
CoO/CoP-NC	1M KOH	$\eta_{10}=178$	88	16
Ce-CoP	1M KOH	$\eta_{10}=81$	69	17

References

1. C. F. Li, H. B. Tang, J. W. Zhao and G. R. Li, *J. Mater. Chem. A* 2023, **11** (11), 5841–5850.
2. R. D. Shi, Y. T. Li, X. X. Xu, X. Wang and G.B. Zhou, *Adv. Funct. Mater.* 2024, **34** (51).
3. M. X. Chen, Y. Y. Zhang, R. Wang, B. Zhang, B. Song, Y. C. Guan, S. W. Li, and P. Xu, *J. Energy Chem.* 2023, **84**, 173–180.
4. K. T. Le, N. N. T. Pham, Y.-S. Liao, A. Ranjan, H.-Y. Lin, P.-H. Chen, H. Nguyen, M. Y. Lu, S. G. Lee and J. M. Wu, *J. Mater. Chem. A* 2023, 3481–3492.
5. S. Diao, T. Wang, W. Kuang, S. Yan, X. Zhang, M. Chen, Y. Liu, A. Tan, T. Yang and J. Liu, *Chem. Eng. J.* 2024, 158738.
6. L. Fu, J. Zhou, Z. Zhou, B. Xiao, N. Khaorapapong, Y. Kang, K. Wu and Y. Yamauchi, *ACS Nano* 2023, **17** (22), 22744–22754.
7. Z. Wu, Y. Gao, Z. Wang, W. Xiao, X. Wang, B. Li, Z. Li, X. Liu, T. Ma and L. Wang, *Chinese J. Catal.*, 2023, **46**, 36–47.
8. H. W. Go, T. T. Nguyen, Q. P. Ngo, R. Chu, N. H. Kim and J. H. Lee, *Small*, 2023, **19**, 2206341.
9. J.-B. Chen, J. Ying, Y.-X. Xiao, G. Tian, Y. Dong, L. Shen, S. I. Córdoba de Torresi, M. D. Symes, C. Janiak and X.-Y. Yang, *ACS Catal.*, 2023, **13**, 14802–14812.
10. X.-C. Meng, J. Luan, Y. Liu, Y.-S. Sheng, F.-Y. Guo, P. Zheng, W.-L. Duan and W.-Z. Li, *J. Mater. Chem. A*, 2024, **13**, 627–637.
11. S.-L. Xu, R.-D. Zhao, R.-Y. Li, J. Li, J. Xiang, F.-Y. Guo, J. Qi, L. Liu and F.-F. Wu, *J. Mater. Chem. A*, 2024, **12**, 15950–15965.
12. Y. Zhang, B. Chen, Y. Qiao, Y. Duan, X. Qi, S. He, H. Zhou, J. Chen, A. Yuan and S. Zheng, *J. Mater. Sci. Technol.*, 2024, **201**, 157–165.
13. X. Cao, S. Xing, D. Ma, Y. Tan, Y. Zhu, J. Hu, Y. Wang, X. Chen and Z. Chen, *J. Energy Chem.*, 2023, **82**, 307–316.
14. L. Yang, X. Cao, X. Wang, Q. Wang and L. Jiao, *Appl. Catal. B Environ.*, 2023, **329**, 122551.
15. H. Luo, X. Zhang, H. Zhu, K. Zhang, F. Yang, K. Xu, S. Yu and D. Guo, *J. Mater. Sci. Technol.*, 2023, **166**, 164–172.
16. K. Chen, Y. Cao, W. Wang, J. Diao, J. Park, V. Dao, G.-C. Kim, Y. Qu and I.-H. Lee, *J. Mater. Chem. A*, 2023, **11**, 3136–3147.
17. M. Li, X. Wang, K. Liu, Z. Zhu, H. Guo, M. Li, H. Du, D. Sun, H. Li, K. Huang, Y. Tang and G. Fu, *Adv. Energy Mater.*, 2023, **13**, 2301162.